

# THE HYDRAULIC ROLE OF ELBOWS IN RECTANGULAR DUCTS OF HVAC DISTRIBUTION SYSTEMS ANALYSED BY CFD

*Marija LAZAREVIKJ<sup>\*1</sup>, Zoran MARKOV<sup>1</sup>, Valentino STOJKOVSKI<sup>1</sup>*

<sup>\*1</sup> Ss Cyril and Methodius University in Skopje, Faculty of Mechanical Engineering - Skopje, 1000  
Skopje, Republic of North Macedonia

\* Corresponding author; E-mail: marija.lazarevikj@mf.edu.mk

*Ducts with rectangular cross-section are widely used in HVAC (heating, ventilation and air conditioning) distribution systems applied to residential, commercial and industrial buildings where round elements can't be used. Usual practical problem is calculating the required pressure drop to drive the air flow for a given duct geometry at a certain flow rate, for which the total hydraulic losses should be obtained. Friction losses in ducts depend on their size, flow capacity and construction material, while minor losses are caused by changes in flow stream direction, expansions or contractions, fittings and valves. The installation of elbow in a channel can induce larger losses due to local flow separation and swirling secondary flow.*

*Viscous incompressible flow of air in the ducts was modelled and simulated. Hydraulic losses in cascade connected straight rectangular sections by three elbows are evaluated with the application of Computational Fluid Dynamics (CFD). Rectangular ducts which have the same hydraulic diameter but differ according to the lengths of their straight sections were being analysed. The numerically obtained loss coefficients were compared with available theoretical data and show good agreement especially in a selected range of Reynolds number. A conclusion is drawn from the comparative analysis that the lengths of the straight sections between the elbows significantly influence the duct hydraulic resistance because of the contribution to the velocity profile uniformity. Moreover, during the separate analysis of the elbows, it is detected that the elbow position in the system is an influencing parameter on the elbow loss coefficient.*

Key words: *rectangular duct, elbow, hydraulic resistance coefficient, CFD*

## 1. Introduction

Many engineering branches where fluid flow takes place require knowledge of resistance to flow in processes of design and operation. Among them are the air conditioning and ventilation systems for which the required power to drive the flow needs to be determined.

Air ducts of ventilation plants in industrial use are usually composed of very long straight pipes and/or relatively short pipelines abound in fittings and branches which makes them complex fluid systems. Their shape can be round, square, rectangular or oval. Rectangular ducts, being lower for the same cross-sectional area, enable lower storey heights while maintaining standard flow velocities [1].

Deficiencies in duct design can result in systems that operate incorrectly, produce inadequate air flow rates or are expensive (increased energy) in terms of investment and operation. Efforts need to be directed towards improving flow conditions and reducing the local fluid resistance of the fittings in the ventilation ducts. It is essential that the fluid resistance of these systems is properly calculated. The resistance coefficients can be given in the form of convenient expressions which can be used in a design analysis of fluid networks. Alternatively, they can be depicted as a functional dependence on the main governing parameters which is practical due to the possibility of graphical representation. In general, the hydraulic resistance coefficient depends on the duct geometry (dimensions, configuration, shape), properties of the material of construction (surface roughness etc.), properties of the fluid (density and viscosity), fluid flow regime etc.

A typical problem to practically solve is the pressure drop needed to drive the flow at a desired flow rate of a fluid with certain physical properties for a given duct geometry with added components such as elbows. Elbows are basic duct fittings which are used to change flow stream direction. Minor losses from elbows are usually measured experimentally and correlated with the flow parameters. The elbow loss coefficient depends on the elbow angle, the curvature ratio and the Reynolds number. Knowledge of elbow loss coefficient is important for accurate calculation of pressure loss of ventilation ducts, so that the ventilating fan is suitably designed.

Fully turbulent flow through curved conduits and channels with local components has been intensively studied by applying theoretical and experimental approaches. In recent years, the emergence of experimental techniques and numerical simulation methods, such as particle image velocimetry and computational fluid dynamics (CFD), has deepened the understanding of the flow fields inside ducts, especially the flow field characteristics and resistance effect of elbows on ducts. Thus, the elbow loss coefficient can be estimated experimentally by physical model measurements or with numerical simulations. The research so far is focused on loss coefficients and secondary flow in channels with elbows.

Zmrhal and Schwarzer [2] compared the results of CFD simulations of ventilation duct elbows with generally accepted published data. While the results published by Idelchik [32] in his extensive work show a similar trend as the simulation results, some data published in German literature [4] cannot be recommended for practical calculation. Liu W. et al. [5] compared the predicted loss coefficient of a duct elbow with the corresponding experimental data from the literature (coefficients have been obtained using experimental measurements according to AHSRAE Standard 120), concluding that the standard  $k$ - $\epsilon$  model and Reynolds stress model could accurately predict the loss coefficient. dos Santos et al. [6] numerically investigated the round elbow loss coefficient at different Reynolds numbers and proposed an equation to describe the relationship. Smyk et al. [7] performed CFD analysis of circular duct with single elbow at Reynolds numbers range of 500 to 100 000 using the  $k$ - $\omega$  turbulence model to investigate pressure losses and Reynolds number influence on the stream separation point shift in the elbow. According to their findings, the calculated minor loss coefficient was similar to the literature values at  $Re > 20000$  and the impact of secondary flow decreased with Reynolds number increasing. Röhrig et al. [8] numerically studied the turbulent flow through a 90-degree pipe with elbow at Reynolds numbers between 14000 and 34000 using LES model and RANS models. Their results were successfully validated against experimentally obtained data. The superiority of LES over RANS was shown, however, at the cost of significant increase in computational effort. Jurga et al. [9] investigated flow through a 90-degree circular pipe bend using

RANS model and considering turbulence anisotropy, validated by comparing axial velocity profiles to previous published experimental data. It was found that the swirl intensity of the secondary flow is a strong function of the of the elbow curvature radius and a weak function of the Reynolds number. Dutta et al. [10, 11] came to the same conclusion using unsteady RANS approach showing the  $k-\epsilon$  turbulence model performs reasonably well. Slug flow in horizontal elbow was experimentally and numerically studied by Cao et al. [12] using the multiphase VOF model and  $k-\epsilon$  turbulence model. Zahedi and Rad [13] experimentally and numerically investigated air–water slug flow in pipe of four 90-degree elbows with different curvature radii and an identical rectangular cross-section. Among other parameters, they analyzed the influence of curvature on velocity and pressure distribution, turbulence and swirling intensity using the VOF and SST  $k-\omega$  model. They concluded that increasing the curvature radius leads to both turbulent and swirling intensity decrement. Weissenbrunner et al. [14] presented a surrogate model for predicting velocity profiles downstream of single elbow and double elbows of circular pipe, using the Spalart–Allmaras turbulence model while considering curvature radius and distance between the elbows as variable parameters. Cuming [15] gives a solution of the Navier-Stokes equations for the flow of a viscous incompressible fluid through curved pipes of different sections i.e., elliptic, rectangular, square and circular in order to theoretically investigate the secondary flow. Characteristics of secondary flow appearing in a straight rectangular duct were extensively described by Stankovic et al. [16], while analyzing fundamentally significant experimental and theoretical studies for mathematical modeling and numerical computations, so as examining the physical mechanisms that generate secondary flow.

According to the literature review, most of the studies focus on air flow in circular ducts with single or double elbow, analyzing the impact of Reynolds number and curvature radius on flow characteristics. This paper studies incompressible viscous air flow through a rectangular duct with three 90-degree elbows, instead of the commonly analyzed circular ones with one or two elbows. The main emphasis is on minor and friction pressure losses represented by the total hydraulic resistance coefficient for such system. Moreover, while investigating the influence of a wider range of Reynolds number on the resistance coefficient, this research work explores the dependency of pressure losses on elbow spacing. The role of elbow's position in the system is shown to be influencing the total resistance coefficient besides them having the same dimensions.

## **2. Methods and materials**

The presented methodology describes the analytical calculation of loss coefficient which offers utilization of the numerical simulations results in practice. The specific case of rectangular channel with three 90-degree rounded elbows is examined.

### **2.1. Methodology for calculating total loss coefficient (coefficient of hydraulic resistance)**

Pressure drop is a consequence of friction and local (minor) losses at fluid flow in pipe. These losses are irreversible transformation of mechanical energy into heat. Friction losses are caused by fluid viscosity and occur along the entire duct length. Friction losses in ducts depend on air velocity, duct size and material roughness. Minor losses result from flow disturbances due to mounted equipment and fitting that change flow direction (elbows), transitions i.e. sudden area changes or converging/diverging junctions.

The Bernoulli equation for a viscous incompressible fluid flow between two sections at a same elevation, in terms of pressure, is given by:

$$p_1 + \frac{\rho v_1^2}{2} = p_2 + \frac{\rho v_2^2}{2} + \Delta p_{t,1-2} \quad (1)$$

where  $p_1, p_2$  are absolute pressures in the respective sections;  $\rho$  is the density of the incompressible fluid;  $v_1, v_2$  are average velocities in the respective sections;  $\Delta p_{t,1-2}$  is total pressure loss between sections 1 and 2.

Accordingly, the total pressure loss is equal to the total pressure change between the two sections:

$$\Delta p_{t,1-2} = p_{t1} - p_{t2} \quad (2)$$

Total pressure loss is a sum of the friction losses and minor losses between the sections:

$$\Delta p_{t,1-2} = \Delta p_f + \Delta p_m = \lambda \frac{L}{D_h} \rho \frac{v^2}{2} + \xi_{loc} \rho \frac{v^2}{2} \quad (3)$$

where  $v$  is the duct mean velocity,  $L$  is the duct length,  $D_h$  is the hydraulic diameter,  $\lambda$  is the friction factor and  $\xi_{loc}$  is a local loss coefficient.

The ratio of the total pressure loss to the dynamic pressure over the duct flow section is called the coefficient of hydraulic resistance or total loss coefficient and can be also represented as a sum of the friction loss coefficient  $\xi_{fr}$  and the local loss coefficient  $\xi_{loc}$ :

$$\xi = \xi_{fr} + \xi_{loc} = \frac{\Delta p_{t,1-2}}{\rho \frac{v^2}{2}} \quad (4)$$

## 2.2. Methodology for calculating total loss coefficient (coefficient of hydraulic resistance) for a three-elbows rectangular channel

The three-elbows rectangular channel consists of inlet straight section with length  $L_0$ , outlet straight section with length  $L_3$ , straight sections between two consecutive elbows with lengths  $L_1$  and  $L_2$ , respectively. The cross section of the channel is a rectangle with width  $a$  and height  $b$ . The radius of the elbow curvature at the central axis is  $R_0$ . The elbow angle is  $\delta$ . The geometry of the system analyzed is given in Fig. 1.

According to the available data from Idelchik [3], for the three-elbows rectangular channel, instead of the hydraulic diameter  $D_h$ , the width  $a$  is taken as the characteristic length and the Reynolds number is expressed as:

$$Re = \frac{\rho v a}{\mu} \quad (5)$$

where  $\mu$  is the fluid dynamic viscosity.

The friction loss coefficient is considering the friction losses occurring in the straight parts between the elbows and in the elbow whose length is  $R_0/a \pi/(180^\circ) \delta$  and calculated as:

$$\xi_{fr} = \lambda \frac{L_1 + L_2}{a} + 3\lambda \frac{R_0}{a} \frac{\pi}{180^\circ} \delta \quad (6)$$

where the friction coefficient for smooth walls is determined by the Blasius's equation for turbulent flow:

$$\lambda = \frac{0,316}{Re^{0,25}} \quad (7)$$

The available data from Idelchik [3] is valid for a three-elbows rectangular duct with the following geometric parameters: relative curvature radius of the axis  $R_0/a=0,75$ ; elbow angle of  $\delta=90^\circ$ ; aspect ratio of  $b/a=0,5$  and ratio  $L_0/a \geq 10$ .

The local loss coefficient according to Idelchik [3] is:

$$\xi_{loc} = 1,5A \quad (8)$$

The factor  $A$  depends on the ratio of the total length between the elbows " $L=L_1+L_2$ " to the duct width  $a$ , as given in Tab. 1.

**Table 1. Values of factor A**

$L/a$	0	1	2	3	4	5
$A$	1,63	1,53	1,16	1,07	1,03	1

The total loss coefficient is determined by:

$$\xi = k_\Delta k_{Re} \xi_{loc} + \xi_{fr} \quad (9)$$

where the roughness coefficient for smooth walls is  $k_\Delta=1$  and the Reynolds number coefficient  $k_{Re}$  is given by Idelchik [3] in Tab. 2.

**Table 2. Values of Reynolds number coefficient**

$Re \cdot 10^{-4}$	1	1,4	2	3	4	6	8	10	14	20	30	40
$k_{Re}$	2,2	2,03	1,88	1,69	1,56	1,34	1,14	1,02	0,89	0,8	0,83	0,9

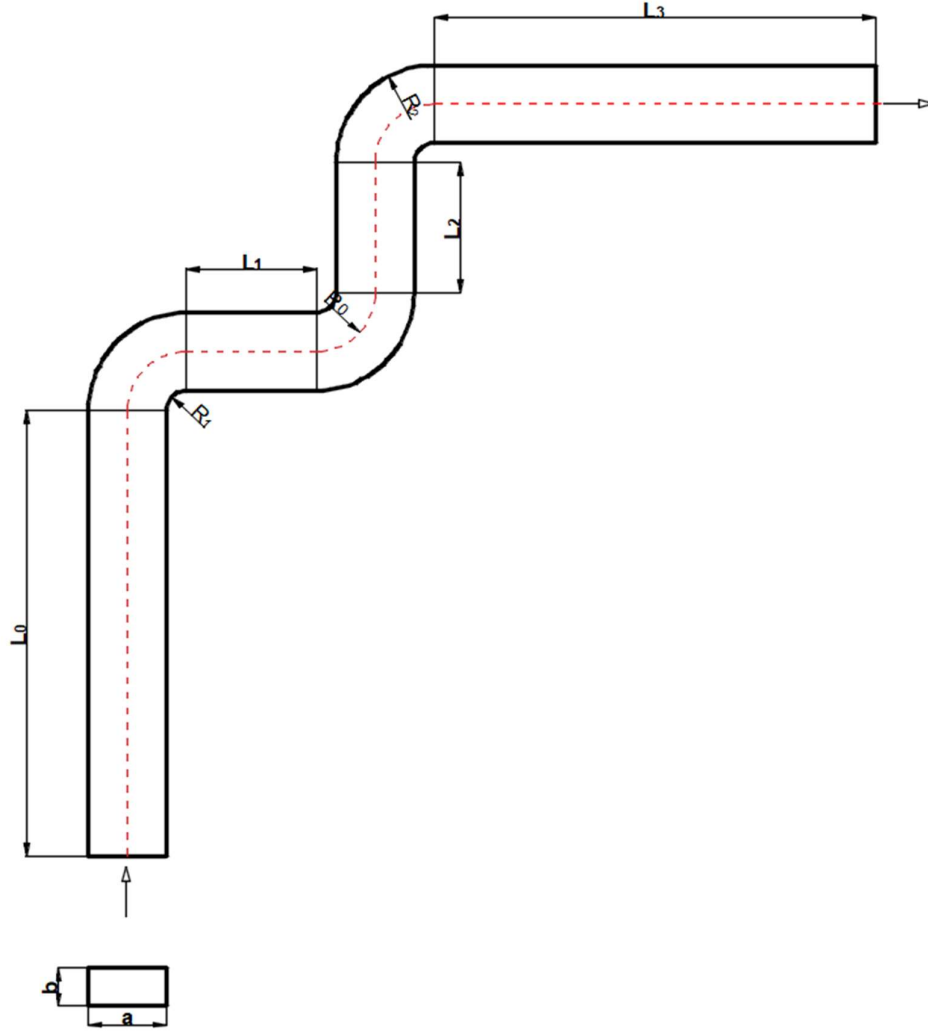


**Figure 1. Schematic of the three-elbow rectangular channel**

### 2.3. CFD methodology

CFD is a numerical method based on solving the Navier-Stokes equations, Eq. (10) and mass conservation law, Eq. (11), respectively:

$$(\mathbf{u} \cdot \nabla)\mathbf{u} = -\frac{1}{\rho}\nabla p + \nu\nabla^2\mathbf{u} + \mathbf{f} \quad (10)$$

$$\nabla \cdot \mathbf{u} = 0 \quad (11)$$

where in Eq. (10) the term on the left is the flow velocity vector (convective term), while the terms on the right are the pressure, the viscous and the body forces, respectively.

### 3. Problem setup

A viscous incompressible flow of air through a three-elbows rectangular channel was analyzed using the software ANSYS Fluent. Three ducts with the same cross section, same lengths of inlet and outlet straight sections, and same elbow geometry, but different lengths of the straight sections between two consecutive elbows were numerically analyzed. The examined ducts and their geometry parameters are summarized in Tab. 3.

**Table 3. Geometry parameters of the investigated channels**

Geom no.	$a$ (mm)	$b$ (mm)	$L_0=L_3$ (mm)	$L_1=L_2$ (mm)	$R_0$ (mm)
1	150	75	1500	300	113
2				375	
3				450	

Decomposition of the computational domain into 7 parts was done to obtain structural numerical grid. The multizone method was used to generate numerical mesh of only hexagonal elements and a boundary layer was placed at the contact of the fluid with the duct walls to properly capture the viscous effects, as shown in Fig. 2.

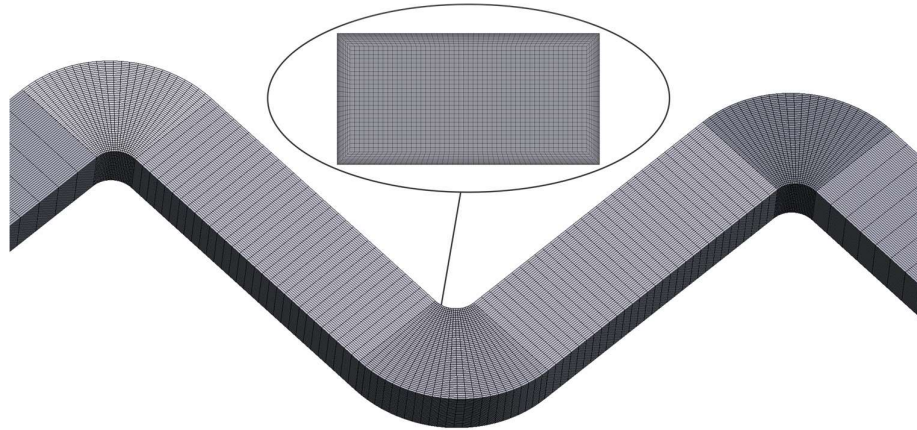


**Figure 2. Numerical mesh**

For resolving turbulence, the 2-equation standard  $k-\epsilon$  model with standard wall functions was used, known for its reliable results for industrial applications. The turbulence model was previously validated by the authors for the case of rectangular channel with one elbow obtaining good agreement between CFD results and experimental data [17]. The SIMPLE solution method was used. Boundary conditions and air properties are given in Table 4.

**Table 4. Processing details**

Boundary type	Details
Velocity inlet	Velocity magnitude: 0.974; 1.363; ..., 38.953 m/s
Pressure outlet	Gauge pressure: 0 Pa
Wall	Stationary wall No slip condition Roughness height 0 mm
Material property	Details
Density	Constant density $\rho=1,225\text{kg/m}^3$

Viscosity	Constant dynamic viscosity $\mu=1,7894 \cdot 10^{-5}$ Pa·s
<b>General</b>	<b>Details</b>
Solver	Pressure based with absolute velocity formation, Steady

## 4. Results and discussion

### 4.1. Flow analysis

Elbows are fittings that change the flow direction. In the straight sections of the duct, the velocity profile is well balanced. When the fluid enters through an elbow, the velocity profile is disturbed (Fig. 3). Because of the elbows, centrifugal forces appear with direction from the center of the curvature to the outer wall resulting in pressure increase (i.e., lower velocity) at the outer wall where a diffuser effect is present and pressure decrease (higher velocity) at the inner wall. When air flows from the curved part into the straight section of the channel, velocity is higher at the outer wall and lower at the inner wall. These effects are present in the case of all Reynolds numbers with a difference in the velocity magnitude.

Flow separation appears at the locations where diffuser effect is present and is characterized by vortices. The separation has higher intensity at the inner walls (straight sections of the duct after every elbow) due to the inertial forces that act in the region of the elbow towards the outer wall. Most of the pressure losses in the duct result from the vortices formation at the inner walls. Fig. 3 shows the velocity vectors distribution in the channel central plane at Reynolds number of 40 000 (40k). In the region of the first elbow, there is no flow separation which means the elbow fulfills its role to change fluid stream direction in conditions when the inlet velocity profile is uniform. The flow is separated at the first elbow outlet. The straight section  $L_1$  is not long enough to obtain uniform velocity profile due to which the flow remains separated at the inlet of the second elbow; the same applies for the third elbow.

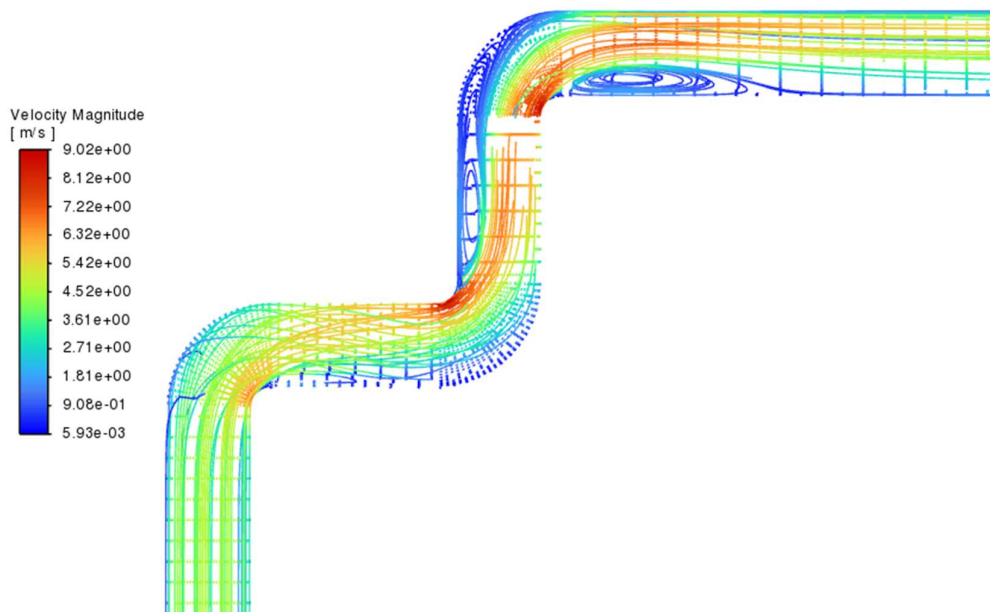


**Figure 3. Velocity distribution in 3-elbows rectangular channel at Re=40k, geometry 1**



The main fluid stream is parallel to the channel axis. The presence of secondary flow in the plane perpendicular to the direction of the main (primary) flow can be seen, which is typical for turbulent flows in straight ducts of non-circular cross-section or curved pipes of any cross-section. The average velocity field includes not only the longitudinal component but also transverse components that create a secondary flow. Secondary flow occurs due to the appearance of centrifugal forces and the presence of boundary layers at the walls. Fig. 4 shows tangential velocity distribution in duct cross-section at the following locations: at the inlet and outlet of the first elbow, second elbow and third elbow, respectively.

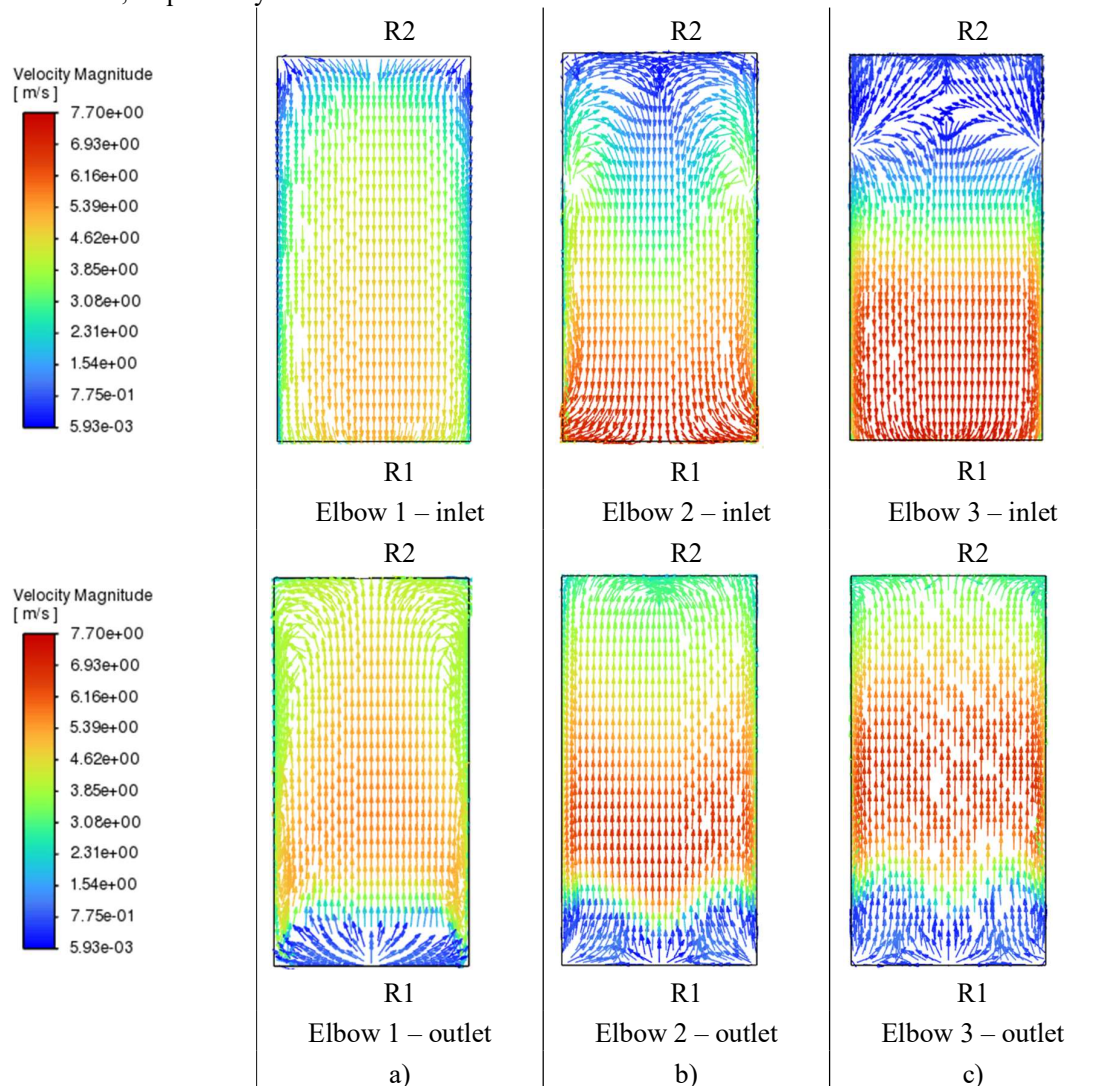


**Figure 4. Tangential velocity distribution at inlet and outlet surfaces of: a) first elbow; b) second elbow and c) third elbow of the 3-elbows channel, geometry 1,  $Re=40k$**

The deformation of the velocity profile causes the local pressure loss. Fig. 5a shows relative velocity profiles at the first elbow inlet and outlet in comparison to the inlet uniform velocity profile at Reynolds number of 40k. It can be seen that the respective velocity profiles are almost the same for different lengths of the straight sections between the elbows. After the fluid passes the elbow, the velocity profile tries to align and it is less disturbed at the elbow outlet. Fig. 5b shows relative velocity profiles at the second elbow inlet and outlet in comparison to the inlet uniform velocity profile at

Reynolds number of 40k. The velocity profile is more deformed at the inlet of the second elbow compared to the first elbow. The length  $L_1$  of the straight section in front of the second elbow is not enough for the velocity profile to align. With increase of the length  $L_1$ , both the inlet and outlet velocity profile of the second elbow is less disturbed, especially in the zone of the outer wall. Fig. 5c shows relative velocity profiles at the third elbow inlet and outlet in comparison to the inlet uniform velocity profile at Reynolds number of 40k. The velocity profile at the third elbow inlet and outlet is even more deformed in the zone close to the outer wall compared to the second elbow. Decrease of length  $L_1$  leads to higher disturbance of the velocity profile at both the elbow inlet and outlet. Reversed flow is obtained at the elbow inlet in the case of the shortest straight sections. The opposite direction of the velocity indicates the presence of reversed flow in the elbow. It can be seen that at each elbow inlet and outlet, the velocity is higher in the region close to the inner wall and lower in the region close to the outer wall.

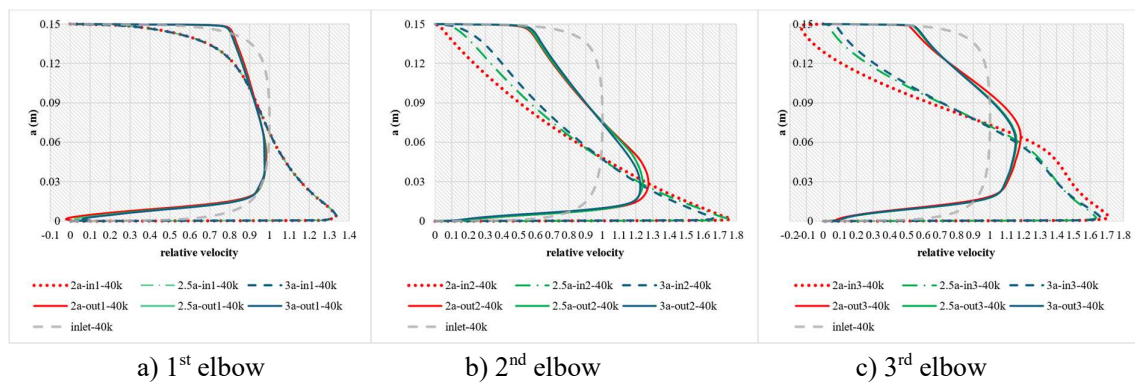


**Figure 5. Velocity profiles at inlet and outlet of 1<sup>st</sup>, 2<sup>nd</sup> and 3<sup>rd</sup> elbow, respectively, at Re=40k for all geometries**

#### 4.2. Analysis of hydraulic resistance coefficients depending on elbows spacing

The total loss coefficient based on the results obtained by CFD analysis ( $\zeta_{CFD}$ ) is calculated by applying equation (4). Numerically obtained results for the dependency of the hydraulic loss coefficient on the flow mode are compared to the available data ( $\zeta_{EXP}$ ). The comparison between the CFD and experimental results is given in Fig. 6a for the cases of longest and shortest straight sections between two consecutive elbows. It can be seen that good agreement is achieved for Reynolds number in the range of 10k-300k. In the case of shortest straight section length ( $2a$ ), the maximum relative error excluding Re=400k was less than 10%, while the maximum relative error for the case of highest straight section length ( $3a$ ) was up to 13%. According to the CFD results, the total loss coefficient decreases with Reynolds number increase. Higher loss coefficient is obtained in the case of shortest straight section ( $2a$ ) at all Reynolds numbers which is explained by the discussion above on the velocity deformation profiles for different section lengths.

Fig. 6b shows the loss coefficient of each elbow in the channel at three different Reynolds numbers, i.e., 40k, 100k and 200k, and for the two different geometries based on the in-between elbows straight sections lengths. As previously discussed in chapter 4.1, the velocity profile in front of and behind the first elbow least deviates from the uniform fully developed velocity profile in the inlet straight section unlike the second and third elbow. That is the reason that the lowest resistance is obtained for the first elbow which is observed to be significantly lower than the second and third

elbow losses. Comparing the hydraulic resistance coefficient of the first elbow in the case of smallest and highest length of straight sections in between the elbows, higher losses are obtained for the geometry with shortest sections. This can be explained by the outlet velocity profile of the first elbow in case of different straight sections lengths where it is seen that reversed flow is more pronounced for the channel with shortest length which contributes to higher losses. In the cases of all three elbows, higher loss coefficient is obtained for the duct with smallest straight sections which are not long enough for the velocity profile to align more. Highest resistance is obtained for the duct with shortest straight sections at the second elbow. Even though reversed flow is more dominant for the third elbow inlet, the velocity profile is more disturbed for the second elbow inlet and outlet. The third elbow has higher losses only for the lowest and highest Reynolds numbers (less than 60k and more than 160k) in the case of channel with longest straight sections. Different hydraulic resistance is obtained even though the elbows have the same geometry because of their different positions in the channel system and different velocity profiles at each elbow inlet and outlet.

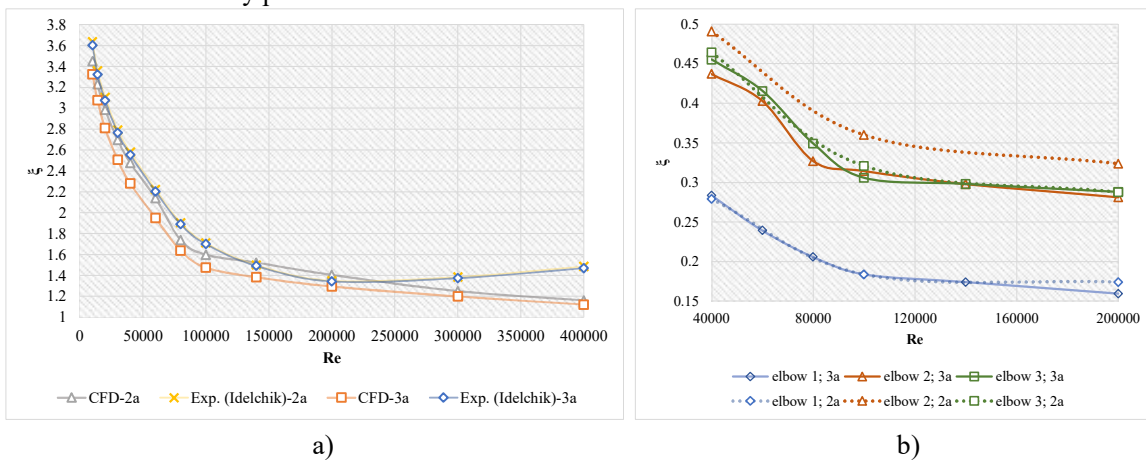


**Figure 6. Comparison of loss coefficient as a Reynolds number function for different channel geometries for: a) whole system; b) separate elbows**

Fig. 7 shows the share in percentage of every component of the three-elbow rectangular channel in the total pressure drop for a given flow mode (defined by the Reynolds number). The percentual share is given sequentially according to the components sequence in the system in direction of the flow, i.e. first elbow, first straight section, second elbow, second straight section and third elbow. It should be considered that all three elbows in the system have the same geometry and size, while the same applies for the two straight sections between them. The obtained results show that:

- The share of hydraulic losses of the elbows in the fluid flow system is different, i.e. the first elbow has the smallest share, while the second elbow has the largest share in the total hydraulic losses
- The share of hydraulic losses of the straight sections in the fluid flow system is different, i.e. the first straight section has lower share in total hydraulic losses than the second straight section.

The uneven contribution to hydraulic losses of different components which are characterized by same geometry and size shows the influence of the element position in the system.

Moreover, the results show that in case of the elbows, increasing the Reynolds number leads to higher share in total hydraulic losses, while in case of straight sections, increasing the Reynolds number leads to lower share in total hydraulic losses.

By increasing Reynolds number, minor losses become more dominant in the distribution of total hydraulic losses. The different participation of individual components in the total pressure drop is

based on the flow conditions in front of the component considered, i.e. due to the flow field disturbance which is shown by the different hydraulic behavior of components identical in terms of geometry and size.

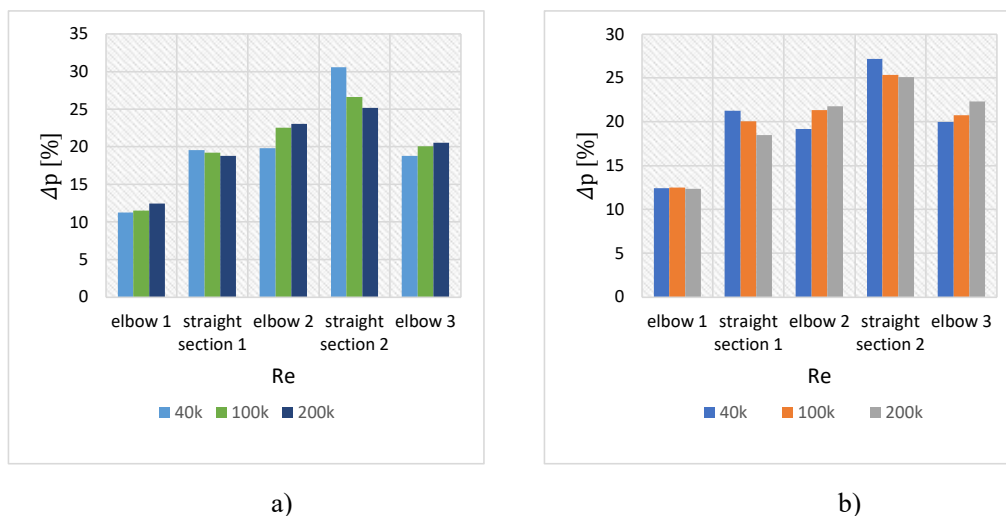


**Figure 7. Share of every component in total pressure drop in the system for: a) geometry 1 (2a); b) geometry 3 (3a)**

## 5. Conclusions

In this paper, numerical simulation of incompressible viscous flow through a 3-elbow rectangular channel was presented. The elbow was chosen as one of the most frequently used fittings in practice, especially in ventilation ducts with rectangular cross-sections. Rectangular channels fit better to building construction – above ceiling and into walls, and they are much easier to install between joists and studs. Three different geometries were analyzed differing on the length of the straight sections between two consecutive elbows. These cases were used to comprehensively describe the most important phenomena that should be taken into account during closed flows, such as secondary flow occurrence and to analyze the dependency of the hydraulic losses on the geometry parameter and the Reynolds number.

The simulation was made with ANSYS Fluent, with the use of the turbulent model k- $\epsilon$ , SIMPLE simulation method, at Reynolds number range of  $Re=10^4 - 40 \cdot 10^5$ . The numerically obtained results are compared with available experimental data. Good agreement is achieved in Reynolds number range of  $10^4 - 30 \cdot 10^5$ . This confirms that the presented methodology can be applied to determine the total loss coefficient of a rectangular channel with three 90 degree elbows.

The study also evaluates how the spacing between elbows affects the pressure losses, It was concluded that the hydraulic resistance coefficient decreases with the Reynolds number increase and decreases with the straight sections' length increase. The influence of this geometry parameter is related to the velocity profile uniformity that contributes to lower resistance. Higher deformations of the velocity profiles lead to larger hydraulic losses. Moreover, it was found that the hydraulic resistance coefficient of elbows with same geometry depends on their position in the fluid flow system. Even with identical dimensions, the positioning of the elbows affects the overall resistance coefficient. The share of every component in the total pressure drop is different: the elbows pressure drop increases with Reynolds number, while the straight sections pressure drop decreases with

Reynolds number. The obtained results for the influence of the system geometry and the flow conditions (defined through  $Re$ ) contribute to the understanding of the influence of the components sequence in the installation. The insights from the results obtained through this research provide a guideline for future engineering designers to consider the system as a whole when predicting hydraulic losses.

#### References

- [1] Smyk, E., Markowicz, M., Szyca, M., Selection of the cross-section area shape of the ducts used in the shelter ventilationsystems - analysis, *Engineering Expert*, No. 1, 2022, pp. 9-17, DOI: 10.37105/enex.2022.1.02
- [2] Zmrhal, V., Schwarzer, J., Numerical simulation of local loss coefficients of ventilation duct fittings, *Proceedings, 11th International IBPSA Conference, Glasgow, Scotland, 2009*, pp. 1761–1766
- [3] Idelchik, I. E., *Handbook of hydraulic resistance* (A. S. Ginevskiy, A. V. Kolesnikov, Eds.; 4th ed. translated by Greta R. Malyavska), Begell House, 2007
- [4] Recknagel, H., Sprenger, E., Schramek, E., *Taschenbuch für Heizung + Klimatechnik 05/06*, Oldenbourg Wissenschaftsverlag, Germany, 2004
- [5] Liu, W., Long, Z., Chen, Q., A procedure for predicting pressure loss coefficients of duct fittings using computational fluid dynamics (RP-1493). *HVAC&R Research*, 18 (2012), 6, pp. 1168–1181, <https://doi.org/10.1080/10789669.2012.713833>
- [6] dos Santos, A. P. P., Andrade, C. R., Zapparoli, E. L., CFD prediction of the round elbow fitting loss coefficient, *International Journal of Mechanical and Mechatronics Engineering*, 8 (2014), 4, pp. 743–747
- [7] Smyk, E., Stopel E., Szyca M., Simulation of Flow and Pressure Loss in the Example of the Elbow, *Water*, 16 Issue13 (2024), 1875; <https://doi.org/10.3390/w16131875>
- [8] Röhrig, R., Jakirlić, S., Tropea, C., Comparative computational study of turbulent flow in a 90° pipe elbow, *International Journal of Heat and Fluid Flow*, 55 (2015), pp. 120-131, <https://doi.org/10.1016/j.ijheatfluidflow.2015.07.011>
- [9] Jurga, A. P., Janocha, M. J., Yin G., Ong, M. C., Numerical Simulations of Turbulent Flow Through a 90-Deg Pipe Bend, *J. Offshore Mech. Arct. Eng.*, 144 (2022), 6, <https://doi.org/10.1115/1.4054960>
- [10] Dutta, P., Nandi, N., Numerical analysis on the development of vortex structure in 90° pipe bend, *Progress in Computational Fluid Dynamics, An International Journal (PCFD)*, 21 (2021), 5, <https://www.inderscience.com/offers.php?id=117466>
- [11] Dutta, P., Chattopadhyay, H., Nandi, N., Numerical Studies on Turbulent Flow Field in a 90 deg Pipe Bend, *J. Fluids Eng.*, 144 (2022), 6: 061104, <https://doi.org/10.1115/1.4053547>,
- [12] Caoa, X., Zhanga, P., Li, X., Li, Z., Zhanga, Q., Bian, J., Experimental and numerical study on the flow characteristics of slug flow in a horizontal elbow, *Journal of Pipeline Science and*

Engineering (2022), 2,

<https://www.sciencedirect.com/science/article/pii/S2667143322000488?via%3Dihub>

- [13] Zahedi, R., Rad, A. B., Numerical and experimental simulation of gas-liquid two-phase flow in 90-degree elbow, Alexandria Engineering Journal 61 (2022), 3, pp. 2536-2550
- [14] Weissenbrunner, A., Ekat, A., Straka, M., Schmelter, S., A virtual flow meter downstream of various elbow configurations, Metrologia 60 (2023) 054002 (15pp),  
<https://doi.org/10.1088/1681-7575/ace7d6>
- [15] Cuming, H. G., The Secondary Flow in Curved Pipes, Aeronautical Research Council Reports and Memoranda No. 2880, London, 1952
- [16] Stanković, B. D., Belošević, S. V., Crnomarković, N. D., Stojanović, A. D., Tomanović, I. D., Milićević, A. R., Specific aspects of turbulent flow in rectangular ducts, Thermal Science 21 (2017), 3, pp. 663–678, <https://doi.org/10.2298/TSCI160201189S>
- [17] Stojkovski, V., Lazarevikj, M., Iliev, V., Dillema about influence of splitter vanes on hydraulic characteristic at rectangular radius elbow, 6th International Scientific Conference on Mechanical Engineering Technologies and Applicatios COMETA, Jahorina, Bosnia and Herzegovina, 2022, pp. 602 – 614

Paper submitted: 30.12.2024

Paper revised: 03.03.2025

Paper accepted: 11.03.2025